JOURNAL OF OPTOELECTRONICS AND ADVANCED MATERIALS Vol. 12, No. 3, March 2010, p. 605 - 609

The effect of laser pulse length upon laser-induced forward transfer using a triazene polymer as a dynamic release layer

J. SHAW STEWART[a,c], R. FARDEL[a,c], M. NAGEL[a], P. DELAPORTE[b], L. RAPP[b], C. CIBERT[b], A.-P. ALLONCLE[b], F. NÜESCH[a], T. LIPPERT[c*], A. WOKAUN[c]

[a]*Empa, Swiss Federal Laboratories for Materials Testing and Research, Laboratory for Functional Polymers, Überlandstrasse 129, 8600 Dübendorf, Switzerland*

[b]*Lasers Plasmas and Photonic Processing Laboratory, CNRS - University of Aix-Marseille, Campus de Luminy - Case 917, 13288 Marseille Cedex 9, France*

[c]*Paul Scherrer Institut, General Energy Research Department, 5232 Villigen PSI, Switzerland*

Laser induced forward transfer (LIFT) is a laser direct write technique based on laser ablation. A UV-absorbing triazene polymer (TP) has been used as a sacrificial dynamic release layer (DRL) to propel other materials forward without damage. The effect of different laser pulse lengths (nanosecond and picosecond) on standard frontside TP ablation and backside TP ablation of aluminium thin films has been studied. Whilst the picosecond ablation causes the shock wave and the flyer to be faster, the ablation rate is considerably lower, suggesting an increase in ablation product energies and a decrease in loss mechanisms. The effect of beam energy homogeneity was seen to be an important factor for good flyer generation.

(Received June 23, 2009; accepted October 7, 2009)

Keywords: Laser forward transfer, Triazene polymer

1. Introduction

Laser induced forward transfer (LIFT) is a positive (involving addition of material) direct-write method [1,2]. It allows controlled transfer of a material from one substrate to another using a laser beam which defines the 2D shape of the deposition. A transparent donor substrate, coated in a transfer material, is irradiated from the "backside" by the laser. Within the transfer material the photon energy is converted into kinetic energy for transfer via photothermal and photochemical ablation processes [3].

A development of this process is to add an intermediary layer whose only role is to absorb the photons and provide the mechanical push to the transfer material [4]. This is commonly called a dynamic release layer (DRL) [5], or an absorbing film [6]. This introduces the possibility that light-sensitive, complex-structured materials may be transferred using LIFT without excessive heat and light damage.

Triazene polymers (TPs) have proved to be excellent materials for the role of DRL. They have a high UV absorption coefficient, and, upon UV laser irradiation, decompose into gaseous fragments which build up pressure and, thus, the thrust for the propulsion of the overlying transfer material layer. They have very low ablation thresholds (~ 25 mJ/cm^2), which means that thermal damage to the transfer material can be kept low. In fact, quantum dots [7], biological cells [8], ceramics [9] and functional organic light-emitting diode (OLED) pixels [10] have all been transferred successfully using this technique.

Triazene polymers were originally tailored for high photon absorption at the 308 nm wavelength of the XeCl excimer laser [11], which is why the bulk of the previous experiments have been conducted using this laser. The TP linear absorption coefficient (α) for 355 nm light is ~ 80 % of that for 308nm, which is still high enough to enable clean ablation. However, a linear optical absorption coefficient obtained from UV-Vis spectroscopy is not really applicable to a dynamic ablation process with temporal and spatial changes in the material properties throughout the pulse duration, particularly considering the movement of the solid-gas interface. For this reason an "effective" absorption coefficient (α_{eff}) is considered, an empirical property dependent on the many material properties that may alter during a laser pulse; these include transient and permanent material modification (i.e. bleaching [12] and incubation [13]) to the film, the different absorption characteristics of the gaseous ablation products [14], and the movement of the solid-gas interface.

The complex mechanism of polymer ablation has been extensively looked at elsewhere, but still has many unanswered questions [3, 15]. TP ablation clearly has a photochemical element to it, in the direct photocleavage of the aryl-triazene chromophore. However, observations have shown that purely thermal decomposition of TP yields almost identical ablation products [16], epitomising the extent that chemical and thermal decomposition of triazene polymers are intertwined.

Recent efforts have been made to analyse the energy pathways in the LIFT process of TPs [17]. Intriguingly,

only about 2 % of the input energy is transferred into the flyer, with ~ 30 % going into the shockwave and the rest lost in other processes (these values vary with fluence). Possible loss mechanisms include mechanical strain upon ejection, gaseous leakage lowering the pressure build-up, and thermal loss into the substrate as well as the rest of the TP film. The thermal loss into the substrate, particularly for frontside ablation of very thin films, has been highlighted by a photothermal model of TP ablation [18].

The experiments undertaken here look both at basic frontside ablation of TP, and at results obtained via backside ablation, propelling thin films of aluminium forward as flyers. Shadowgraphy of these aluminium films flying through the air allows us to quantify the kinetic energy being transferred both to the flyer and the shockwave, which is also visible with shadowgraphy. These experiments have been made using three different laser pulse lengths in an attempt to observe the effects that changing the pulse length has upon TP ablation and LIFT using TP as a DRL. The results will be used as a guide for further study into the mechanism and energy balance of TP ablation.

2. Experimental techniques

The samples were composed of a high-quality quartz glass substrate spin-coated with a layer of triazene polymer (polymer TP-6a in [19]). For backside ablation shadowgraphy studies only, an 80nm film of aluminium was evaporated on top of the TP layer. For frontside ablation, the sample is aligned so that the laser beam impinges upon the TP layer directly, orthogonal to the surface. For the backside ablation experiments, the laser beam irradiates from the opposite direction, through the transparent substrate. The ablated area was kept constant for all of the experiments: a 500 µm square generated by a 2 mm square mask of the laser beam, demagnified by a factor of 4 using an achromatic lens.

In previous studies, the principal laser system that has been used to study laser ablation of TP is the 308nm excimer laser (ns / 308 nm), with a pulse length of 30 ns [20, 21]. The other laser systems used here are both solid-state lamp-pumped Nd:YAG lasers, at the 3rd harmonic wavelength of 355 nm. These have pulse lengths of 5 ns (ns / 355 nm) and 70ps (ps / 355 nm). The aryl-triazene chromophore absorption curve has a peak in the UV which is almost at its maximum at 308 nm, but is about 20 % lower at 355 nm [19]. The bulk of the previous experiments have been done using the ns / 308 nm, and this work expands the ablation data to two more laser systems. The beam energy profile of the excimer is the most homogenous mainly due to its flat-top structure. Both of the Nd:YAG lasers, as well has having Gaussian beam energy profiles, contain hot-spots, but these were minimised as far as possible for the experiments. The beam energy was measured using a pyroelectric energy meter, and attenuated beam energy profiles were measured using a CCD camera.

For the shadowgraphy experiments using the two nanosecond pulse lasers, a pump-probe set-up provided illumination using the fluorescent flash from a cuvette filled with Rhodamine 6G dye, triggered by a time-resolved probe ns laser pulse from a second laser. This stroboscopic illumination creates a time-resolved image on the digital camera with its shutter opened for far longer than the flash of the probe illumination. For the picosecond shadowgraphy experiments a second Nd:YAG laser provided continuous illumination, at 532 nm, for a gated ICCD camera which could be time-resolved to within 20 ns.

Profilometry was used to look at the ablation depth for frontside ablation, as well as to measure the film thickness and roughness. The profiles were obtained using an Ambios XP-1 profiler. Pictures of the ablated spots were taken using a Leica digital camera attached to a Zeiss Axioplan microscope.

3. Results and discussion

3.1 Frontside ablation

Two outcomes of the frontside ablation studies are graphically depicted in Figures 1 and 2: the threshold fluence as a function of film thickness, and the ablation depth for a single pulse (known as the ablation rate) as a function of laser beam fluence, respectively. In both graphs there are clear differences between all three lasers, highlighting that the pulse length has an effect on the TP ablation process. One other variable that may have a significant effect should also be kept in mind: the difference in wavelength between the excimer (308 nm) and Nd:YAG (355 nm).

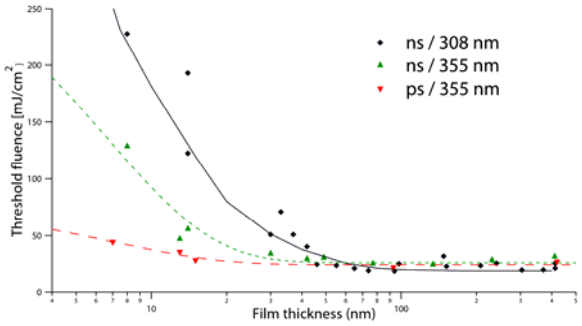

Fig. 1. Threshold fluence for a single pulse as a function of TP film thickness. The error in the threshold fluence is that of the fluence (~ 5 %) plus the error from fitting a range of them (8-10%), giving a total of ~ 15 %. The film thickness variation is ± 5 nm. The solid guideline was made from the model in [18], but the other two lines are exponential fits to guide the eye.

In Fig. 1, while the data points of the ns / 355 nm and the ps / 355 nm were fitted to a simple exponential function to guide the eye, the line fitted to the excimer laser data points was generated from the model proposed by *Fardel et al.* in [18]. This graph is intended to provide a

comparison between the data already fitted to the model and the new data, and to see what aspects of the model may be changed by using shorter pulses. The model is primarily based on a photothermal model for laser ablation, taking into account light absorption changes with depth, and it makes a strong case for thermal diffusion as an important loss mechanism that limits the level of ablation, and increases the threshold fluence for frontside ablation of thin films by heat diffusion energy loss into the substrate. It is note-worthy that the model does not take into account the non-linear processes that affect the thermal diffusion, such as material decomposition during the pulse, or the temperature dependence of material properties such as thermal diffusivity. Nor are photochemical processes taken into account; experimentally these are very hard to differentiate from photothermal reactions as the products are almost identical, but the difference in timescales of photochemical reactions (≤ ps) vs photothermal reactions (ns) may have important implications for the kinetics of the ablation process if photochemical processes are significant.

Fig. 1 shows the increase in the threshold fluence at low TP film thicknesses. The degree to which the threshold fluence increases is the most notable difference between the different lasers. Less obviously, there is also a distinct variation in the thickness at which the onset of threshold fluence increase starts. The threshold fluences do not show much variation for films thicker than ~ 100 nm. Due to the higher TP linear absorption coefficient, it might be expected that the 308 nm threshold fluence would be lower than that for the 355 nm lasers. Despite the graph suggesting this may be the case, the possible error in the threshold fluence value makes it impossible to conclude this. While the experimental error of the fluence is a maximum of ± 5 %, the error for the threshold fluence is likely to be larger, as that depends on additional factors such as the number of data points used for the fit, and their range, the reliability of all those fluences being accurate, the quality of the fit equation used. Figure 2 gives an example as to how the threshold fluence is calculated using equation 1 as the fit. This uncertainty increases the threshold fluence error by ~ 10 %. The spread in the film thickness measurements is up to 5 nm, and so negligible at large thicknesses, but quite significant for the films below 100 nm.

Changes in thermal diffusion into the substrate due to the shorter heating time could account for the lowering in threshold fluence at low film thicknesses with shorter pulse length. Nevertheless, even if thermal loss into the substrate has significant influence upon films under 100 nm thick, the effect will not be significant for thicker films until the ablation depth approaches the film thickness (within the thermal diffusion length). These results are interesting for fundamental TP ablation understanding, but it should be remembered that the results are only for frontside ablation. Backside ablation has a completely different configuration, with the ablation of the Triazene starting with that in contact with the quartz substrate, and so the thermal diffusion processes will be different.

Fig. 2 shows the ablation rate as a function of fluence, using TP films which were roughly 420 nm thick. The threshold fluence for 308 nm (~ 21 mJ/cm^2) irradiation appears lower than for both of the 355 nm laser irradiation (~ 30 mJ/cm^2), but figure 1 showed that the experimental scatter in the threshold fluence means that this cannot be concluded. The 308 nm laser appears to ablate deeper craters than both of the 355 nm lasers for the fluence range of the graph. However, differences in the curve's shapes suggest that the ns / 355 nm curve will intersect the ns / 308 nm curve well before the whole film is ablated. The ps / 355 nm curve appears to be approaching an asymptotical ablation depth far below the curves of the two ns lasers. The shapes of the curves give the effective absorption coefficients by fitting them to an ablation equation modified for ablation from Lambert-Bouguer's law of absorption [22]:

$$d = \frac{1}{\alpha_{eff}} \ln \frac{\Phi}{\Phi_{th}} \tag{1}$$

where d is the ablation depth, Φ is the fluence, Φ_{th} is the threshold fluence, and α_{eff} is the effective absorption coefficient. The fits give a higher α_{eff} for the ps / 355 nm (~ 8.6 x 10^4 cm^{-1}) than the ns / 355 nm (~ 6 x 10^4 cm^{-1}) laser. The ns / 308 nm laser has an effective absorption coefficient in between (~ 7 x 10^4 cm^{-1}). These values for the ns pulses suggest that the difference in TP linear absorption coefficient at the different wavelengths does effect the effective absorption coefficients. Evidence to the contrary has been shown in [23] where TPs with different chromophore densities, and therefore different TP linear absorption coefficients, have the same ablation rates. However, this evidence does not necessarily count against the results here, because α was altered by changing the material's absorption properties in [23], rather than by using different wavelengths, as in this study.

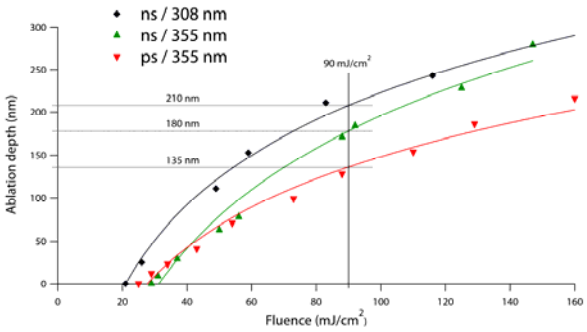

Fig. 2. Ablation depth versus fluence for frontside ablation of 420 nm thick TP films. The error in measured ablation depth is about ± 5 nm, and the standard deviation in the measured fluence is between 3 and 5 %. The curves are fitted according to the empirical relation given in equation 1. The guidelines at 90 mJ/cm^2 are reference values for the ablation rates in Fig. 3.

The ps / 355 nm ablation rate, with its high α_{eff}, is

noticeably lower than both of the nanosecond lasers in figure 2. The greater effective absorptivity need only be linked to the shorter pulse length; a reduction in thermal diffusion may be one explanation for this, but it is by no means the only one. The shorter pulse time means that the movement of the solid-gas interface will be kept to a minimum by the kinetics of the ablation and this means that an extension of the optical penetration depth, expected for nanosecond pulses by the interface movement during the pulse, would not be as prevalent. Another effect, which can occur at picosecond timescales, is possible two-photon and multiple-photon absorption which would increase the effective absorptivity of the TP [24]. Overall, the higher TP absorption for picosecond pulses points to higher energy gaseous products, possibly smaller fragments with higher kinetic energy, generated over a shorter time, along with reduced energy losses.

3.2 Backside ablation and shadowgraphy

The flyers are shown in figure 3, produced by backside ablation, at a laser fluence of 90 mJ/cm^2, of samples with a 350 nm layer of TP coated with 80 nm of aluminium. The clearest observation is that ps / 355 nm ablation generates faster flyers and shockwaves than for either of the two nanosecond laser systems, which both have the same flyer and shockwave velocities as each other within experimental error. The other interesting trend is the decrease in flyer quality as the pulse length shortens.

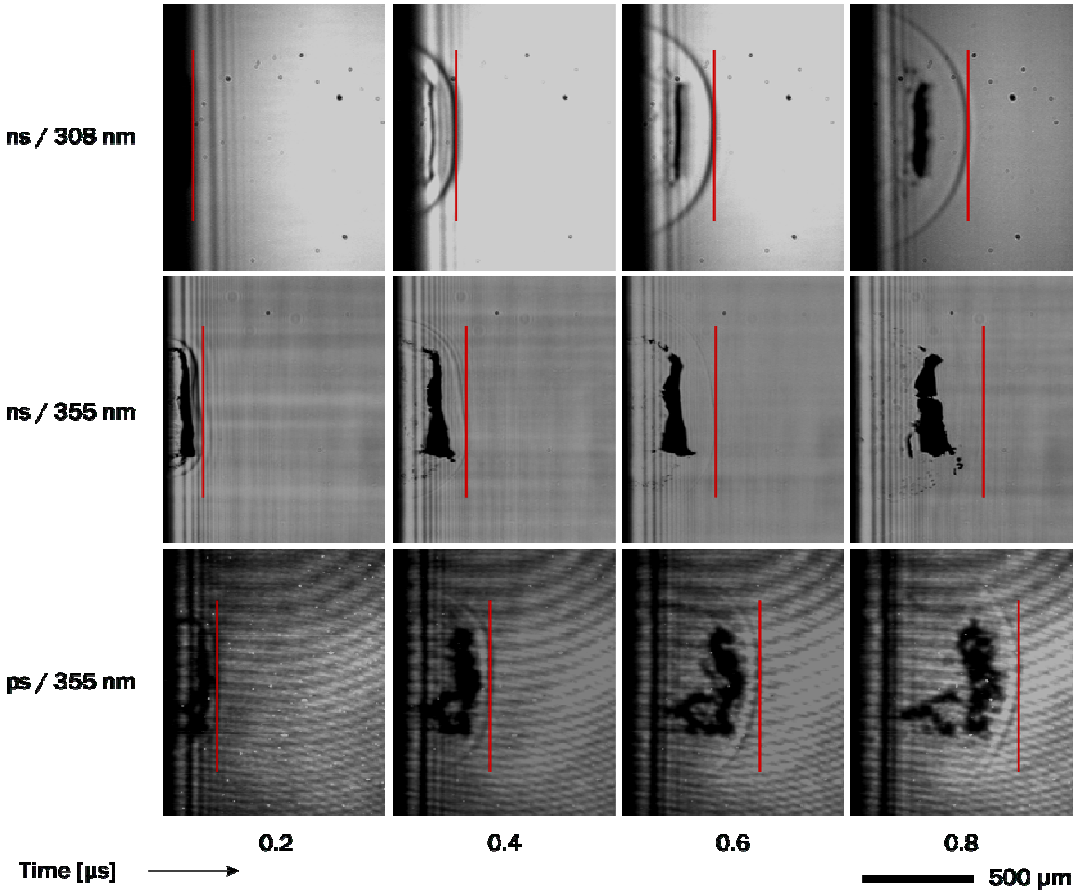

Fig. 3. Time-resolved shadowgraphy images of backside ablation using samples comprising 350 nm TP coated with 80 nm Al, irradiated at 90 mJ/cm^2. The line on each image highlights the shockwave position.

It is usually assumed that ablation rates measured by frontside ablation will be the same for backside ablation [20]. This means that the shockwave speed should be directly associated to the volume of TP ablated by frontside ablation. The ablation depth for each laser, at 90 mJ/cm^2, is shown on Fig. 2; this clearly shows that the picosecond pulse has a lower ablation rate, and yet still propels the projectile at a far greater velocity than for the nanosecond pulses. The fact that a smaller volume of TP is being ablated, and yet there is a greater build-up in gas pressure, means that the ablation products are smaller, with more kinetic energy. On top of this, the increased pressure build up could be the result of a reduction in post-ablation energy losses, such as gas leaks due to the speed of gas build up, or pre-ablation energy losses, such as thermal diffusion. These reductions in energy losses can be neatly explained by the shorter pulse length shortening the timescale over which all energy losses can take place.

The velocity of the ps / 355 nm shockwave, in figure 3, has been calculated to be about 30 % faster (above mach

2) than the shockwaves of the ns pulses, giving an increase in the shockwave kinetic energy of 70 %. Assuming all the energy comes from the laser at a fluence of 90mJ/cm^2, this means that the proportion of total input energy in the shockwave has increased from about 1/3 for the 308 nm irradiation [17] to 1/2 for picosecond 355 nm irradiation. This equates to a reduction in energy losses of at least 20 % of the input energy at 90 mJ/cm^2 for the 70 ps pulse when compared to the ns pulses.

The flyer quality decrease is the result of a combination of poorer beam energy homogeneity of the Nd:YAG lasers than the excimer and the explosive ablation at the picosecond pulse lengths. In addition to lacking any hot spots, unlike both of the Nd:YAG lasers, the flat-top nature of the excimer beam enables a more homogenous energy profile to be obtained than the Gaussian Nd:YAG beams. Due to the nature of the beam energy profiles the beam energy homogeneity can be said to be a major reason why the flyers are more fragmented for the Nd:YAG lasers, particularly the ps laser which was the least homogeneous by far.

4. Conclusions

Using picosecond pulse lengths to irradiate TP films causes significant changes to the ablation process when compared to the more commonly studied nanosecond pulse ablation. The shorter pulse length decreases the ablation threshold, lowers the ablation threshold increase that is observed with films thinner than 100nm, ablates a shallower depth per pulse above a critical fluence, propels the shockwave and flyer faster, and appears to create a more fragmented flyer. These effects, except for the latter, are all mainly the result of the picosecond laser's pulse length timescale which creates higher energy ablation products by increasing the effective absorption of the triazene polymer and reduces losses due to the whole process happening faster. Finally, the homogeneity of the beam energy profile has been observed to be vital for the generation of good flyers.

References

[1] J. Bohandy, B. F. Kim, F. J. Adrian, Journal of Applied Physics, **60**, 1538 (1986).
[2] C. B. Arnold, P. Serra, A. Piqué, Mrs Bulletin, **32**, 23 (2007).
[3] N. M. Bityurin, B. S. Luk'yanchuk, M. H. Hong, T. C. Chong, Chemical Reviews, **103**, 519 (2003).
[4] W. A. Tolbert, I. -Y. Sandy Lee, M. M. Doxtader, E. W. Ellis, D. D. Dlott, Journal of Imaging Science And Technology, **37**, 411 (1993).
[5] D. P. Banks, K. Kaur, R. Gazia, R. Fardel, M. Nagel, T. Lippert, R. W. Eason, EPL (Europhysics Letters), **83**, 38003 (2008).
[6] B. Hopp, T. Smausz, N. Barna, C. Vass, Z. Antal, L. Kredics, D. B. Chrisey, Journal of Physics D: Applied Physics, 38 833 (2005).
[7] J. Xu, J. Liu, D. Cui, M. Gerhold, A. Y. Wang, M. Nagel, T. K. Lippert, Nanotechnology, **18**, 025403 (2007).
[8] A. Doraiswamy, R. J. Narayan, T. Lippert, L. Urech, A. Wokaun, M. Nagel, B. Hopp, M. Dinescu, R. Modi, R.C.Y. Auyeung, D. B. Chrisey, Applied Surface Science, **252**, 4743 (2006).
[9] K. S. Kaur, R. Fardel, T. C. May-Smith, M. Nagel, D. P. Banks, C. Grivas, T. Lippert, R. W. Eason, Journal of Applied Physics, **105**, 113119 (2009).
[10] R. Fardel, M. Nagel, F. Nüesch, T. Lippert, A. Wokaun, Applied Physics Letters, **91**, 061103 (2007).
[11] T. Lippert, A. Wokaun, J. Stebani, O. Nuyken, J. Ihlemann, Angewandte Makromolekulare Chemie, **206**, 97 (1993) .
[12] T. Lippert, L. S. Bennett, T. Nakamura, H. Niino, A. Ouchi, A. Yabe, Applied Physics A, **63**, 257 (1996).
[13] S. Küper, M. Stuke, Appl Phys A, **49**, 211 (1989).
[14] M. Hauer, T. Dickinson, S. Langford, T. Lippert, A. Wokaun, Applied Surface Science **197**, 791 (2002).
[15] T. Lippert, J. T. Dickinson, Chemical Reviews **103**, 453 (2003).
[16] O. Nuyken, J. Stebani, T. Lippert, A. Wokaun, A. Stasko, Macromolecular Chemistry and Physics, **196**, 751 (1995).
[17] R. Fardel, M. Nagel, F. Nüesch, T. Lippert, A. Wokaun, The Journal of Physical Chemistry C, **113**, 11628 (2009).
[18] R. Fardel, M. Nagel, F. Nüesch, T. Lippert, A. Wokaun, B. S. Luk'yanchuk, Applied Physics A, **90**, 661 (2008) .
[19] M. Nagel, R. Hany, T. Lippert, M. Molberg, F. A. Nüesch, D. Rentsch, Macromolecular Chemistry and Physics, **208** 277 (2007).
[20] R. Fardel, M. Nagel, F. Nüesch, T. Lippert, A. Wokaun, Applied Surface Science **255**, 5430 (2009).
[21] R. Fardel, M. Nagel, F. Nüesch, T. Lippert, A. Wokaun, Applied Surface Science **254**, 1322 (2007).
[22] J. E. Andrew, P. E. Dyer, D. Forster, P. H. Key, Applied Physics Letters **43**, 717 (1983).
[23] R. Fardel, P. Feurer, T. Lippert, M. Nagel, F. Nüesch, A. Wokaun, Applied Surface Science **254**, 1332 (2007).
[24] H. Fujiwara, T. Hayashi, H. Fukumura, H. Masuhara, Applied Physics Letters, **64**, 2451 (1994).

*Corresponding author: thomas.lippert@psi.ch